Hyperspectral Reflectance for Preliminary Identification of Degraded Soil Zones in Industrial Sites: A Screening Tool before Undertaking Ground-Based Investigations

Amitava Dutta[1]*, Rashi Tyagi[2], Shilpi Sharma[1,2] & Manoj Datta[3]

[1] School of Interdisciplinary Research (SIRe), IIT Delhi, New Delhi, India
[2] Department of Biochemical Engineering and Biotechnology, IIT Delhi, New Delhi, India
[3] Department of Civil Engineering, IIT Delhi, New Delhi, India
*Corresponding Author's email: srz218571@iitd.ac.in

Abstract
The study aims to explore the potential of next-generation satellite hyperspectral imaging systems for screening and predicting surface soil contamination/degradation in heavily industrialized areas, by exploiting various spectral indices and signature matching techniques. The study area comprised of 07 industrial tailing ponds, 05 material dump sites, 07-08 coal storages, 05 power plants and 07-08 industrial units including three aluminum factories. The soil moisture content, desertification status, salinity index, clay or fine material content, heavy metal indices, vegetation health status, and stress levels were predicted from continuum-removed spectral reflectance values. Results indicated the presence of water in 02 tailing ponds, high salinity, and desertification values in most of the ponds and dump sites, clay boundary liner along four ponds, high heavy metal indices along three ponds and all dump sites, highly stressed vegetation near all tailing ponds and coal dump sites, and pollutants in nearby water channels. The results set a strategy for the initial identification of priority areas for ground-based investigations. The approach emphasizes the potential of satellite hyperspectral imaging as a screening tool for providing an alternative rapid methodology to monitor industrial hubs.

Keywords: Hyperspectral imaging, soil contamination, industrial hubs

Introduction

The mapping and monitoring of industrial byproducts or residues through their mineral composition at various sites, specifically in developing countries, is a topic of increasing interest as high risk factors for land, water, and air pollution. The various industrial byproducts or residues can also be reused and recycled under the framework of a cyclic economy, such as reducing the consumption of virgin raw materials in construction industry, landfilling and road development, agricultural activities etc. The characteristics of industrial byproducts or residues in tailing ponds or dump sites are mostly determined through extensive ground sampling and subsequent wet chemistry/lab analysis. These processes are expensive, time-consuming, tedious, and sometimes subjective. Monitoring diversified large industrial hubs through traditional techniques is unsuitable for a fast-developing economy like India. Remote sensing technologies, specifically satellite hyperspectral imaging, could provide rapid, precise, and economical monitoring of various industrial hubs for their impact on the surrounding environment, and identification of policy gaps at the regional level in this regard.

Hyperspectral imaging, also known as imaging spectroscopy can precisely identify the surface materials through their fingerprints, like spectral signatures. Undoubtedly, in the last three decades, hyperspectral imaging has proven its' capability as a powerful and precise tool for environmental monitoring by diagnosing characteristic spectral signatures of various materials (Marion et al., 2018). It allowed researchers to exploit distinct spectral absorption features, their relative strength, shape etc., for precise identification and mapping the spatial distribution of various pollutants (Swayze et al., 2000; Mars et al., 2003; USGS, 2005; Pascucci et al., 2012). Researchers adopted diversified approaches such as spectral indices, usually developed using normalized band ratioing at absorption features (Asadzadeh et al., 2016), spectral signature library matching techniques (Clark et al., 2003; Pascucci et al., 2012; Marion et al., 2018), physically based approaches such as modified Gaussian model (Sunshine et al., 1990; Sunshine et al., 1993; Brossard et al., 2016), and more recently, machine learning/deep learning techniques are used for characterization of industrial and mining tailing using hyperspectral imageries.

Satellite hyperspectral remote sensing-based mapping and monitoring of industrial byproducts or residues/pollutants through spectral signature analysis is still in infancy, especially in the Indian scenario. It is primarily due to the nonavailability of open domain satellite platform for hyperspectral imaging post Hyperion era (NASA E0-1 satellite, decommissioned in early 2017) and require specialized manpower and optimized processing algorithms. The present study attempts to fill this gap by exploiting next-generation German DLR EnMAP satellite hyperspectral datasets and specialized image processing techniques. To the best of our knowledge, this is the first report on the use of hyperspectral data from a satellite platform for industrial by-products or residues/pollutants mapping in India. The study aims to identify various soil and vegetation stress parameters by exploiting satellite hyperspectral spectral indices and spectral signature-based identification of industrial byproducts or residues/pollutants in a highly industrialized area in India. The approach emphasizes the potential of satellite hyperspectral imaging as a screening tool for providing an alternative rapid methodology to monitor industrial hubs.

Materials and Methods

Study Area: The study site is Jharsuguda Industrial Area in Odisha, located at 21.7840 N, 84.0313 E, in the eastern central part of India. The industrial hub is spread over an area of approx. 30 Km x 30 Km, along the northern and eastern banks of Hirakud Reservoir with well-connected road and railway networks. Many aluminum factories, steel, and power industries, mining industries, quarrying sites, tailing ponds etc. are in the industrial hub. In the hyperspectral imagery of 19 April 2023, three aluminum plants with associated infrastructures (power plants, coal and material dumps, tailing ponds etc.), few power and metallurgical & steel plants, and numerous small industries, dumping and quarrying sites were identified using Google Earth and Open Street Maps (Figure 1). The diversified nature of the industrial hub, and its large spatial extent, provide a unique opportunity to map and monitor industrial pollutants in nearby areas using hyperspectral imaging, which otherwise, through traditional ground surveying methods, would have taken months to generate a synoptic view with a huge cost burden.

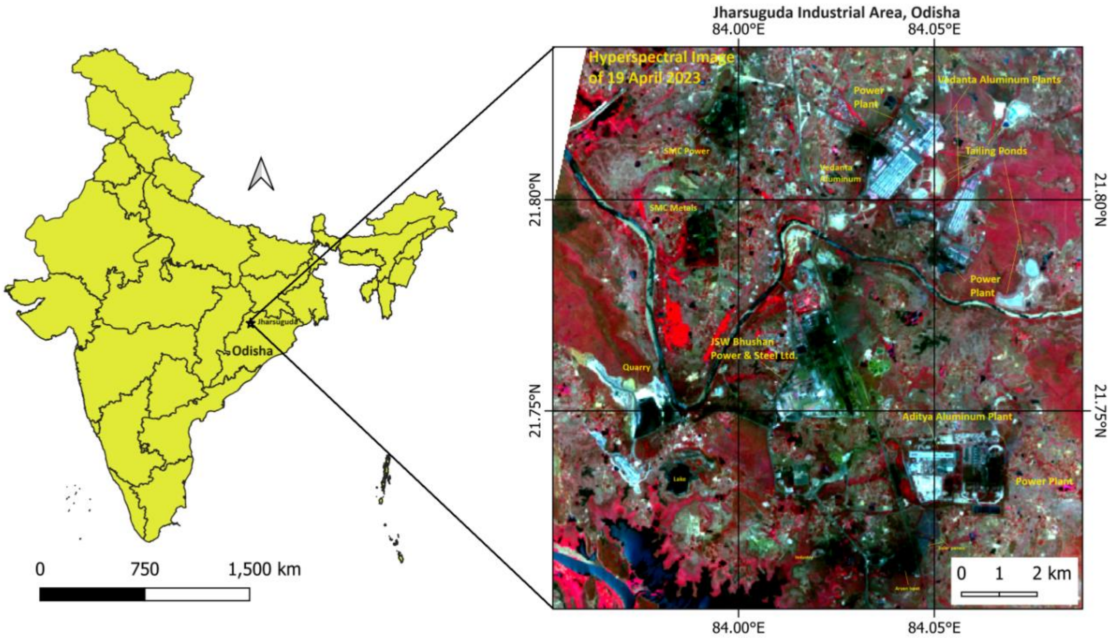

Fig. 1 Jharsuguda Industrial Area, Odisha, showing the locations of various industrial units, tailing ponds and nearby waterbodies from the hyperspectral imagery of 19 April 2023.

Datasets and Materials: German DLR EnMAP satellite hyperspectral image of 19 April 2023 with 212 bands (0.4-2.5 µm) covering the Jharsuguda Industrial Area, Odisha, was downloaded from https://eoweb.dlr.de/egp/ and exploited for various hyperspectral indices generation, and spectral analysis for material identification and pollutants mapping. In the absence of ground survey datasets for accuracy assessment, high resolution Google Earth multispectral imageries, Sentinel-Hub analytics and ground pictures were consumed.

*Methodology:*After atmospheric and bad band corrections, EnMap hyperspectral imagery was exploited to generate six selected spectral indices: water index, salinity index, desertification index, soil clay content, iron oxide index, and vegetation stress index. The water index map was generated to highlight the moisture content within the industrial tailing ponds to indicate possible fresh deposits. Salinity and desertification indices together would highlight the soil health status in terms of acidification or various salt contents. Since soil clay content and organic matter have strong positive correlations with soil heavy metal concentration, clay and iron oxide indices were also incorporated for soil health analysis. The vegetation stress map based on greenness (Atmospherically Resistant Vegetation Index), canopy water content (Water Band Index), and plant light use efficiency (Anthocyanin Reflectance Index) for photosynthesis, was generated exploiting continuum removed spectra from hyperspectral image. These six indices individually and collectively identified the priority areas for ground-based investigations. The various spectral indices, formulae, utility, selected range, and references are summarized in Table 1.

In parallel to calculation of spectral indices, machine learning-based spectral signature matching algorithms: Adaptive Coherence Estimator (ACE), Spectral Angle Mapper (SAM), Constrained Energy Minimization (CEM) and match filtering (MTMF), were also verified in the context of efficient detection of industrial byproducts or residues in surrounding areas. Since the study site comprised at least three large aluminum extraction plants (Figure 1), and ~85% of the total bauxite produced worldwide is processed into aluminum, it is assumed that for these plants also, most likely, bauxite is used as raw material. Bauxite, which is formed by intense leaching in tropical and subtropical regions by laterization process, is a mixture of the aluminum hydroxides gibbsite, boehmite, diaspore, iron oxides goethite and hematite, along with kaolinite clay, and small amounts of titanium dioxide (Ghrefat et al. 2021). Bauxite is also used in cement, metallurgical, and chemical industries. The above hypothesis of bauxite being used as the raw material in these aluminum plants was tested with the presence of Bauxaline® or red mud dust (alkaline) residue of aluminum production, red gypsum (similar color residue), bauxite (ore), and Alumina (product) at the site exploiting spectral signature matching techniques.

Table 1 Summary of various spectral indices exploited in the present study.

Spectral Index	Formula	Utility & Range	Reference
Water Index (NDWI)	(R_864nm–R_1245nm)/(R_864nm+R_1245nm)	Analyze the water presence in tailing ponds (>0)	Gao (1996)
y Index (SI)	√(R_436.99nm*R_630.32nm)	Soil salt concentration mapping (>1300)	Kumar et al. (2015)
Desertification Index (NMDI)	R_860nm - (R_1640nm–R_2130nm)/ R_860nm + (R_1640nm–R_2130nm)	Soil desertification measure (>0.9)	Wang et al. (2007)
Soil Clay Content	Calculate continuum removed absorption depth between 2120 nm and 2250 nm.	Clay mineral content (>0.17)	Chabrillat et al. (2011)
Iron Oxide Index	(R_660nm)/(R_485nm)	Estimation of heavy metal oxides in soil (>2)	Segal (1982)
Vegetation Stress Index	ARVI= NIR – [Red-Y (Blue-Red)]/ NIR + [Red-Y (Blue-Red)] WBI=(R_970nm)/(R_900nm) ARI2= R_800nm (1/R_550nm–1/R_700nm)/	Relative assessment of vegetation stress in a scale between 1 and 9 (>5)	ENVI (https://www.nv5geospatialsoftware.com/docs/AgriculturalStressTool.html)

Results

Results of the two parallel steps i.e., spectral indices generation, and spectral matching, adopted in the study are separately described in the subsequent paragraphs.

Spectral Indices:

Water Index: In Normalized Difference Water Index (NDWI) defined by Gao (1996), positive values highlight the pixels with water presence. In the present study area, high water presence was detected in tailing pond-1 (P1 in Figure 2b) inside the aluminum processing plants. Out of the five tailing ponds maintained by Vedanta (P-1 to P-5; Figure 2a), pond-1 had water presence, and pond-5 had relatively higher moisture content compared to the other four tailing ponds.

Salinity Index: The soil salinity, a measure of soil degradation, is determined by Salinity Index (SI) developed by Kumar et al. (2015). In the study area, most of the places showed moderate-low salinity, except the five material dump sites (S1-S5) and the tailing pond-1, where severely saline soils were detected (>1500-1600) using SI (Figure 2c).

Desertification Index: NDMI developed by Wang et al. (2007), can highlight the pixels with very low moisture content leading to higher soil desertification. In consistence with previous sub-section findings, at the tailing pond-1, higher desertification index values (>0.9) were detected. In addition, the tailing ponds 3 and 5 also indicated higher positive values in their western parts (Figure 2d).

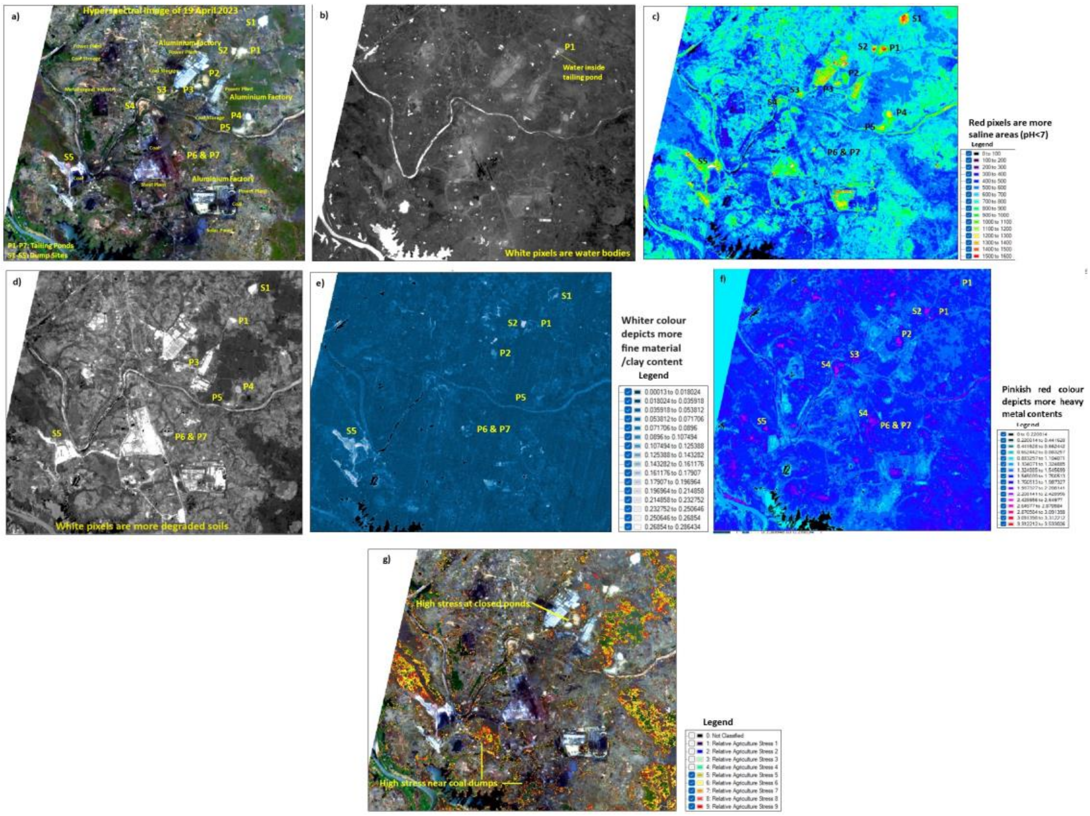

Fig. 2 (a) Overall location of tailing ponds and material dump sites. **(b)** Water index map. **(c)** Soil salinity index map, **(d)** Desertification index map. **(e)** Soil clay content map. **(f)** Iron oxide index. **(g)** Vegetation stress map (relative).

Soil Clay Content: As suggested by Chabrillat et al. (2011), soil clay content measure calculates continuum removed absorption depth difference between 2120 nm and 2250 nm, and highlights the pixels with higher clay content. For material dump sites 2 and 5 (S-2 & S-5), higher clay index values >0.2 were observed, indicating the presence of finer materials in higher quantities at these sites. Tailing pond-2 also had index values >0.13, the highest among all tailing ponds, indicating more clay content than other ponds (Figure 2e). Incidentally, the clay index also highlighted the clay liner barrier along the boundaries of five tailing ponds (P1-P5) in aluminum mills.

Iron Oxide Index: Developed by Segal (1982), the iron oxide ratio estimates the heavy metal oxide contents in soil. For the study area, >2 index values were observed for four material dump sites (S-2 to S-5) and at three tailing ponds (P-2, P-6, and P-7) (Figure 2f).

Vegetation Stress Index: The vegetation stress index map is a combined score of plant greenness (ARVI), canopy water content (WBI) and light use efficiency (ARI) indices and significantly high (scores 8 and 9 on a scale of 1-9) stress was observed along the boundary regions of mining tailing ponds and coal dumping sites (Figure 2g).

Spectral Matching: Standard spectral signature libraries of Bauxaline® or red mud dust (alkaline) residue from aluminum production, red gypsum (similar color residue as Bauxaline®, but waste material of titanium dioxide extraction from ilmenite and rutile), bauxite (ore), and alumina (finish product) were collected from literature (Marion et al. 2018), resampled and filtered at EnMAP spectral bands before feeding into the system. Subsequently, the same target signatures were used in machine learning algorithms (ACE, CEM, SAM, MTMF) for detection in hyperspectral imagery. The reference signature of Bauxaline®, the waste product of aluminum extraction, was automatically detected by ACE algorithm at eleven places of 30 Km x 30 Km area covered in the hyperspectral imagery, although the other target detection algorithms could not perform reasonably. High-resolution Google Earth multispectral images of concurrent/nearby time indicated the presence of red dust at the same places (Figure 3). Therefore, it can be summarized that spectral signature matching techniques successfully detected the aluminum waste products from satellite hyperspectral imagery. It gives an idea about the nature of the industrial activities at the industrial hub. The bauxite ore and finished product alumina were not detected from satellite hyperspectral image-based signature matching techniques, as probably these materials are being kept under the sheds due to their economic values, while like Bauxaline® waste products are stored in the open.

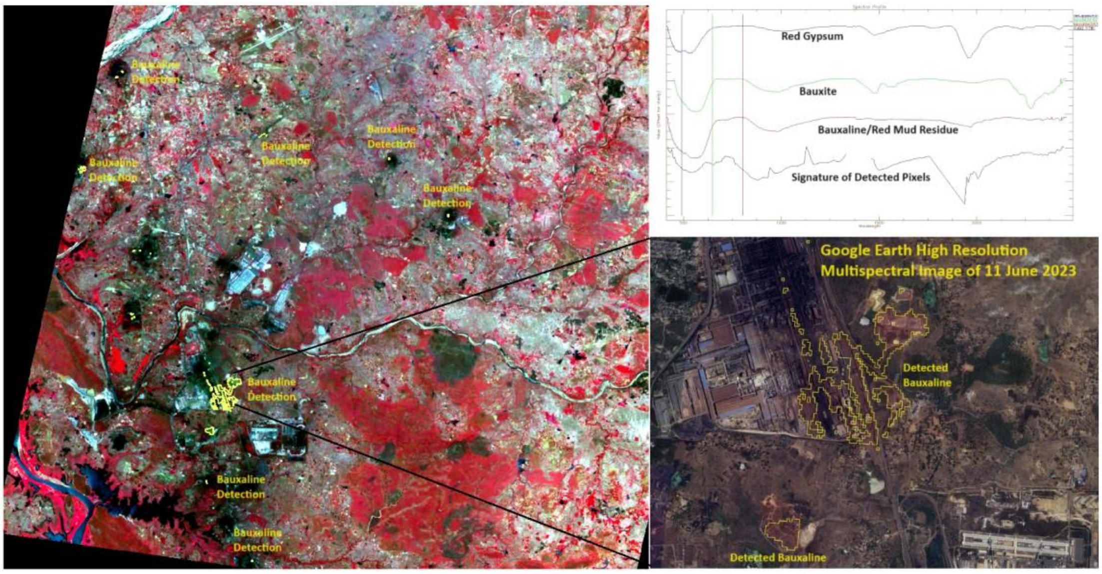

Fig. 3 Signature matching results. **(a)** location of Bauxaline deposits. **(b)** Spectral signatures. **(c)** Detection results plotted on high-resolution Google Earth multispectral imagery for better perception.

Discussion

The values of the three spectral indices (NDWI, SI, and NDMI) clearly highlight that the industrial tailing pond-1 located within aluminum mill complexes had highly saline and degraded surface materials/soils with the presence of water, which in turn may indicate that it is operational. Similarly, the material dump site-2, located adjacent to the tailing pond-1, had high salinity, large clay/fine content, and high concentrations of heavy metals as discerned from hyperspectral imagery. This prioritizes the place for ground-based investigations, the first objective of the present study. In addition, tailing ponds 2, 6, and 7 also showed high values in heavy metal index. Samples from these three tailing ponds need to be collected and tested in a laboratory for further corroboration of the findings. The vegetation stress map (combined score of greenness, canopy water content, and light use efficiency) depicted high stress near the coal dumping sites, indicating possible high dust pollution in nearby areas.

Spectral signature matching techniques identified dumping of Bauxaline®/red mud residue at tailing ponds 6 and 7 along with ten other places. The locations were validated with Google Earth high-resolution multispectral images, which indicates about 80-90% accuracy in detection results. Moreover, there were many places with similar red dust as discerned from high resolution multispectral images, but these were not detected from hyperspectral images. It also highlights the unique capability of hyperspectral imaging technology, although these findings are pending ground verification. The detected Bauxaline®/red mud residue in imagery is reportedly highly alkaline, and generally composed of iron, silica, alumina, titanium, calcium minerals, sodium salts, and trace amounts of various elements such as barium, boron, cadmium, chromium, cobalt, gallium, lead, scandium, and vanadium (Marion et al. 2018) and must be contained in engineered storage facilities. Dry Bauxaline®/red mud residue has a high potential for air pollution if kept in the open. Therefore, scientific management of Bauxaline®/red mud residue should be followed.

Conclusions

The present study highlights the efficiency of next-generation hyperspectral satellites for rapid, precise, and economical monitoring of complex industrial hubs in rapidly growing nations like India. It delineates the priority areas for further ground-based investigations. The methodology presented in the article could be adopted for policy decision-making and implementation at regional level.

Acknowledgements

Authors are grateful to German-DLR space agency for providing the En-MAP satellite hyperspectral imagery free of cost. RT acknowledges the DST-INSPIRE fellowship received from Department of Science and Technology, Government of India.

References

Asadzadeh, S., & de Souza Filho, C. R. (2016). A review on spectral processing methods for geological remote sensing. International Journal of Applied Earth Observation and Geoinformation, 47, 69–90.

Brossard, M., Marion, R., & Carrére, V. (2016). Deconvolution of SWIR reflectance spectra for automatic mineral identification in hyperspectral imaging. Remote Sensing Letters, 7, 581–590.

Chabrillat, S (2011) HYSOMA: an easy-to-use software interface for soil mapping applications of hyperspectral imagery. 31st EARSeL Symposium, 30 May-02 June, Prague, Czech Republic.

Clark, R. N., Swayze, G. A., Livo, K. E., Kokaly, R. F., Sutley, S. J., Dalton, J. B., McDougal, R. R., & Gent, C. A. (2003). Imaging spectroscopy: Earth and planetary remote sensing with the USGS Tetracorder and expert systems. Journal of Geophysical Research: Planets, 108, 5.1–5.44.

Gao, B., C. (1996). NDWI: A Normalized Difference Water Index for remote sensing of vegetation liquid water from space. Remote Sensing of Environment, 58, 257-266.

Ghrefat, H., Mutairi Y., A., ElAraby, H., Galmed, M., & Mohamed, E. (2021). Using reflectance spectroscopy and Advanced Spaceborne Thermal Emission and Reflection Radiometer data to identify bauxite deposits in vicinity of Az Zabirah, northern Saudi Arabia. Arabian Journal of Geosciences, 14, 820.

Kumar, S., & George, K., J. (2015). Hyperspectral remote sensing in characterizing soil salinity severity using SVM technique - a case study of alluvial plains. International Journal of Advances in Remote Sensing and GIS, 4(1), 1344-1360.

Marion, R., & Carrère, V. (2018). Mineral mapping using the automatized gaussian model (AGM)—application to two industrial French sites at Gardanne and Thann. Remote Sensing, 10, 146.

Mars, J. C., & Crowley, J.K. (2003). Mapping mine wastes and analyzing areas affected by selenium-rich water runoff in southeast Idaho using AVIRIS imagery and digital elevation data. Remote Sensing of Environment, 84, 422–436.

Segal, D. (1982). Theoretical basis for differentiation of ferric-iron bearing minerals, using Landsat MSS data. Proceedings of symposium for remote sensing of environment, 2nd Thematic Conference on Remote Sensing for Exploratory Geology, Fort Worth, TX pp. 949-951, 1982.

Sunshine, J. M., Pieters, C. M., & Pratt, S.F. (1990). Deconvolution of mineral absorption bands: an improved approach. Journal of Geophysical Research: Planets, 95, 6955–6966.

Sunshine, J. M., & Pieters, C. M. (1993). Estimating modal abundances from the spectra of natural and laboratory pyroxene mixtures using the modified gaussian model. Journal of Geophysical Research: Planets, 98, 9075–9087.

Swayze, G. A., Smith, K. S., Clark, R. N., Sutley, S. J., Pearson, R. M., Vance, J. S., Hageman, P. L., Briggs, P. H.; Meier, A. L.; Singleton, M. J.; et al. (2000). Using imaging spectroscopy to map acidic mine waste. Environmental Science & Technology, 34, 47–54.

USGS. (2005). Remote sensing for environmental site screening and watershed evaluation in Utah mine lands—east Tintic mountains, Oquirrh mountains, and Tushar mountains; U.S. Geological Survey scientific investigations report 2004-5241; USGS: Denver, CO, USA.

Yuting, W (2019) Tailings reservoir disaster and environmental monitoring using the uav-ground hyperspectral joint observation and processing: a case of study in Xinjiang, the belt and road. IEEE international geoscience and remote sensing symposium, 9713-9716, 28 July-02 August, Yokohama, Japan.

Citation

Dutta, A., Tyagi, R., Sharma, S., Datta, M. (2024). Hyperspectral Reflectance for Preliminary Identification of Degraded Soil Zones in Industrial Sites: A Screening Tool before Undertaking Ground-Based Investigations. In: Dandabathula, G., Bera, A.K., Rao, S.S., Srivastav, S.K. (Eds.), Proceedings of the 43rd INCA International Conference, Jodhpur, 06–08 November 2023, pp. 181– 188, ISBN 978-93-341-2277-0.